

Mathematical modeling of the submarine permafrost long-term dynamics and gas hydrate stability zone in the Siberian Arctic shelf*

V.V. Malakhova

Abstract. Results of the mathematical modeling of the dynamics of the submarine permafrost and the methane hydrate stability zone in the sediment of the East Siberian Arctic shelf are presented. The thickness of permafrost on the shelf is 175–320 m for the geothermal heat flux 60 mW/m^2 according to the results of experiments. The permafrost modeling indicates to the fact that after the seafloor warming from 1948 to 2012 the permafrost upper boundary deepens for only about 1–20 m. The thawing permafrost dynamics is more sensitive to the magnitude of the heat flux than to the bottom water temperature changes. A possible existence of close and open taliks in the permafrost in the Laptev Sea is shown.

Keywords: subsea permafrost, submarine permafrost, the East Siberian Arctic shelf, methane hydrate stability zone

Introduction

The Arctic is especially affected by climate warming, and therefore is of the keen scientific interest. The arctic regions show the highest rates of warming in recent years and continue to be a hot spot of climate changes [1]. A recent decrease of the perennial sea ice during the summer season over the Arctic shelves was a bright indicator of this process [2]. Also, the observed data reveal climatic changes occurring in the atmosphere, on land and in the ocean. Most of such impacts have already been detected and are likely to be found in the future [3,4]. This paper explains how the effects of changing climate may have influence on the submarine permafrost. Climatic changes are likely to cause warming of the bottom sea water and deeper seasonal thawing of permafrost.

The extensive Arctic Shelf can play an important role in the methane cycling because of a huge storage of organic matter buried in permafrost, which can be involved in the modern biogeochemical cycles subject to warming. The East Siberian Arctic Shelf (ESAS), consisting of the Laptev and the East Siberian seas, represents the shallowest and broadest shelf region of the entire World Ocean. The ESAS is underlain by the relic off-shore submarine permafrost in an environment that is favorable for the stability

*Supported by Integration Project No. 109 of SB RAS.

of gas hydrates [5,6]. During the last glacial maximum, the global sea levels fell by over a hundred meters, with a result that the shallow seas of the shelves became a dry land, which allowed the permafrost to develop there. Both models and geophysical data support the existence of the subsea permafrost in large areas of the Arctic shelves down to a water depth of about 100 m.

Availability of the sub-sea permafrost on the Arctic shelf is till now one of the discussed questions, as the geological studies in this region are very limited. Only a few drilling transects within the Arctic Seas have been studied. A review of the sub-sea permafrost measurements for the Siberian shelf can be found in [7]. In the Laptev coastal zone, the subsea permafrost was found within many sites: Khatanga Bay, Mammoth Tusk Cape, around the Lena and Yana Deltas, Bykovsky Peninsula, Buor-Khaya Bay and around the Big and Small Lyakhovski Islands [7].

The research into the state and dynamics of the submarine permafrost is of a great interest due to a potential industrial development of the offshore gas fields and, also, has important climatic significance. The sub-sea relict permafrost is thought to contain large volumes of CH_4 in the form of gas hydrates at depths of up to several hundred meters. In [8] estimate 3.75×10^2 Gt C in methane hydrates just on the East Siberian Arctic Shelf (ESAS). Degradation of gas hydrates resulting from climate changes could increase a flux of CH_4 to the atmosphere. The stability of the sub-sea permafrost with a changing climate depends directly on the magnitude of changes in water temperature and salinity, air temperature, sea-ice thickness, and seabed stability. The state of permafrost in the Arctic is a potential key to understanding whether methane, stored in the permafrost-related gas hydrate, can release to the atmosphere. Methane, a very radiative active trace gas and therefore affecting the global warming, is produced in the thawing permafrost and released into the atmosphere.

The dissolved methane concentrations in the ESAS water during the summers of 2003 to 2013 show a widespread supersaturation over large spatial scales [8]. The horizontal and vertical methane distributions in the observational data indicate to a sedimentary source which is likely to be associated with thawing of the underwater permafrost and release of gas from the shallow Arctic gas hydrate. It has been hypothesized that enhancing the methane transport to the atmosphere realeased from methane hydrates offshore is due to the formation of open taliks, caused by the current warming.

To study the correct distribution of the permafrost thickness on the ESAS, the mathematical modeling is widely used. Numerous studies by scientists [5–7, 9–11] have documented the existence of the subsea permafrost in the near-shore areas of the Arctic Ocean. The created models significantly differ in the underlying assumptions, giving different results regarding

the age, thickness and temperature of the submarine permafrost. The key question to be answered is the presence of open taliks through which gases can reach to the bottom water and of thawing areas in which the methane production is enhanced. Two basic mechanisms of the sub-sea permafrost degradation are present in models: the geothermal heat flux and the surface warming. The bottom water temperature plays a significant role in the current state of submarine permafrost, because it specifies the frozen soil thawing depth. The submarine permafrost can thaw fully or partially if the temperature of the bottom water is positive. In [12], it is shown that an extended summer-ice free period in the Laptev Sea shelf has led to an increase of the bottom water temperature since the mid-1980s.

This paper attempts to answer this question with the help of numerical calculations of the ESAS permafrost stability and the permafrost-related gas hydrate stability zone (GHSZ), using bottom layer temperature data from 1948 to 2012, based on the regional model “the Arctic Ocean-North Atlantic”. In this paper, we also examine the role of the soil conditions, in particular, of a geothermal heat flux, on the simulated submarine permafrost thickness. The main objectives of our research are to evaluate a potential effect of the recent climatic warming on the subsea permafrost degradation and to determine possible sources of methane in the high-latitude subsea permafrost regions.

1. Material and methods

1.1. Description of permafrost model. The study area includes the shelves of the Laptev and the East Siberian seas with depths up to 100 m. Whenever the sea levels dropped worldwide during cold stages, [6] the ESAS areas with a water depth up to 10–100 m were obtained. The marine transgression brings about a change from sub-aerial to submarine boundary conditions for permafrost. When the sea level is low, permafrost is formed in the exposed shelves under cold sub-aerial conditions. When the sea level is high, permafrost becomes degraded in the submerged shelves under relatively warm boundary conditions.

The mathematical modeling was applied in order to study the distribution and thickness of the offshore permafrost. The simulation of the offshore permafrost thickness evolution used in this study is based on the one-dimensional solution of Stephan’s problem with mixed boundary conditions [6, 13]. The model takes into account the latent heat at the phase change boundary through the adjustment of the volumetric heat capacity when the sediment temperature approaches 0°C . At each shelf point, we simulate the temperature field of the space containing the permafrost zone by a 1D heat equation with a phase change:

$$C_T \frac{\partial T_S}{\partial t} = \frac{\partial}{\partial z} \left(\lambda_T \frac{\partial T_S}{\partial z} \right), \quad C_M \frac{\partial T_S}{\partial t} = \frac{\partial}{\partial z} \left(\lambda_M \frac{\partial T_S}{\partial z} \right), \quad (1)$$

$$\left(\lambda_T \frac{\partial T_{S1}}{\partial t} - \lambda_M \frac{\partial T_{S2}}{\partial t} \right) = LW_S P \frac{\partial X}{\partial t}. \quad (2)$$

We exploit the Dirichlet and the Neumann boundary conditions at the ground surface and at the depth:

$$z = H_{ij} : \quad T_S = T_B, \quad z = H_{ij} + 1000 \text{ m} : \quad \lambda_T \frac{\partial T_S}{\partial z} = Q_T. \quad (3)$$

In these equations, t is the time; T_S is the sediment temperature ($^{\circ}\text{C}$); L is the volumetric latent heat (J/m^3); W_S is the liquid pore water fraction in the sediments (m^3/m^3); λ_T and λ_M are the thermal conductivity of sediments (W/mK) for unfrozen and frozen ground materials, respectively; C_T and C_M are the volumetric heat capacity of sediments ($\text{J}/\text{m}^3 \text{ K}$) for unfrozen and frozen ground materials, respectively; $\frac{\partial T_{S1}}{\partial t}$ and $\frac{\partial T_{S2}}{\partial t}$ are temperature gradient out and into of the element containing the phase change boundary; $\frac{\partial X}{\partial t}$ is the rate of movement of the phase change boundary; P is soil porosity; H_{ij} is the sea water depth (m) in the point (i, j) ; T_B is the surface ground temperature; and Q_T is the geothermal heat flux (mW/m^2).

Equation (2) describes the rate by which the latent heat is lost or gained by each element containing the phase change boundary, [6]. The geothermal heat flux at the low boundary of sediments was set as 45–100 mW/m^2 [6, 9]. The physical constants in the heat diffusion equation are specified following [6]. A uniform thermal conductivity $\lambda_T = 2.0 \text{ W}/\text{mK}$ and $\lambda_M = 2.1 \text{ W}/\text{mK}$ is assumed for the unfrozen and frozen subsurface materials, according to [14]. A uniform water content of 20 % in the sediments is assumed to participate in the phase change. We assumed the simulated permafrost to be a homogeneous ground material. We follow the commonly assumed point of view [6] and suppose that the ground does not contain salt. Mathematical implementation and the code are borrowed from [13]. The time-dependent change of the temperature is calculated by an explicit finite difference scheme. The model was run with the day time step and grid spacing was 0.5 m in the vertical direction.

1.2. The paleogeographic scenario. Transgressions and regressions of the ocean, which occurred in the past, have affected the development of permafrost on the Arctic shelf. The duration of the transgression/regression cycle, air temperature, the ocean bottom water temperature, the geothermal heat flux are some of the most important factors affecting the sub-sea permafrost distribution, [15, 16]. The boundary conditions were selected in accordance with the paleoscenario for the ESAS, which corresponds to the

last glacioeustatic cycle [16]. The modeling of the dynamics of the temperature fields within the shelf was performed for one climatic glacial cycle (i.e., for the last 120,000 years), [9]. According to [9], the paleoscenario for the modeling was derived from the recent ice-core data obtained at the Vostok station in Antarctica [17].

The initial conditions (120 kyr ago) were set proceeding from the assumption of the absence of permafrost on the sea shelf and the stationary temperature distribution with depth [18]:

$$T_S(z_n, 0) = T_S(z_{n-1}, 0) + \frac{\Delta z Q_T}{\lambda_n},$$

where $T_S(z_n, 0)$ is the temperature of the soil of the n th layer, Δz is the thickness of the grid element, Q_T is the geothermal flow and λ_n is the heat conductivity of the n th layer.

We define the surface ground temperature T_B as the temperature at the bottom water layer or as the air temperature, depending on the simulated period:

$$T_B = \begin{cases} T_W & \text{in the case of a transgression period,} \\ T_G + T_V & \text{in the case of a regression period,} \end{cases}$$

where T_G is the present day mean annual ground temperature and $T_G = -12^\circ\text{C}$ at the coast of the Dmitry Laptev Straite, [9, 16], T_V is the air temperature anomaly reconstructed from the Vostok ice core data for the last 120 kyr [17], T_W is the temperature at the bottom water layer. When the shelf is inundated, we assume that the ground surface temperature is determined by the ocean bottom water temperature T_W .

One of the difficulties in the sub-sea permafrost modeling is to find the time when the shelf point was flooded during the transgression. According to [15, 18], the ocean transgression began, approximately, 15,000–13,000 years ago. The time for the establishment of the modern sea-level in the Arctic Siberia was about 5,000 years ago. To establish a chronology of the Holocene transgression in the Arctic, a total of 14 sediment cores from the Laptev Sea continental slope and shelf were studied in [18]. On this basis it was estimated that the flooding of the 50, 43, 31, and 0 m isobaths was completed by, approximately, 11.1, 9.8, 8.9, and 5 kyr ago. According to the vertical resolution of the ocean model [20] and the estimates [18], we take that the flooding of the 75, 50, 30, and 0 m isobaths was completed 13, 10, 9, and 5 kyr ago.

1.3. The water masses state. We consider two different periods for the post-transgression bottom water temperature. From the beginning of the ocean transgression 13–5 kyr ago up to 1947, we assume that an average bottom temperature $T_W = -1.5^\circ\text{C}$ in the whole shelf zone. For analyzing

the sensitivity of the subsea permafrost to the recent warming, we consider the monthly average bottom water temperature. From 1948 up to 2012, we have simulated the sediment temperature based on the bottom water temperature with the Arctic Ocean regional model.

The oceanic processes are described using the ocean dynamics numerical model of the world ocean circulation in the region of the Arctic Ocean and Northern Atlantic (AO-NA), [20–22]. The problem is solved with respect to time by a hybrid explicit–implicit scheme with the method of splitting to physical processes and spatial coordinates. The horizontal spacing in the polar grid varies from 50 to 34 km.

Based on the AO–NA regional model, the variability of the Arctic Ocean water masses state was simulated for the period from 1948 to 2012. The analysis of the simulated ESAS sea temperatures variability has shown a positive trend in the bottom temperature, which is in agreement with the observational data [23]. The results obtained demonstrate a warming temperature in the areas affected by the Lena river outflow.

1.4. Simulation of the Gas hydrate stability zone. Gas hydrate is an ice-like solid that is formed in sediments and remains stable at certain pressure-temperature conditions. Gas hydrates in nature contain mostly methane as the trapped gas. It is assumed that methane hydrate concentrates CH_4 by ~ 164 times on a volumetric basis as compared to gas at standard pressure and temperature conditions. Warming a small volume of a gas hydrate could thus release large volumes of gas.

We have also simulated the dynamics of the methane hydrate stability zone. The thickness of GHSZ was calculated applying the pressure-temperature equilibrium of the methane hydrate system, the model of heat transport in soil, bottom-water temperature, and a geothermal gradient. The modeling of GHSZ was based on the use of a general regression expression derived in [24] based on the data from [25]. Limited smoothing in the vicinity of the quadruple point was implemented to allow continuity of the derivatives and smooth phase changes [26].

2. Simulation results

2.1. Subsea permafrost modeling. The results of our simulation show existence of the that offshore permafrost within the vast Arctic shelf in the East Siberia. Figure 1 shows the temporal evolution of the vertical temperature profiles across 600 m below the seafloor, starting from 13 kyr ago until 2012. Calculations of the evolutionary dynamics of the permafrost thickness were made for the geothermal heat flux as 60 mW/m^2 . The lower permafrost boundary varied from 530 to 320 m for the whole simulation

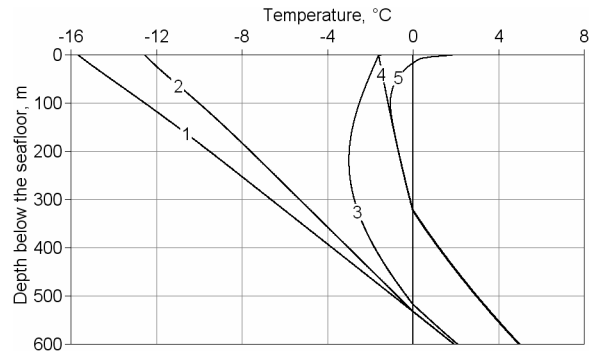


Figure 1. The mean temperature field as a function of depth: (1) for 13 kyr ago, (2) for 9 kyr ago, (3) for 4 kyr ago, (4) for 1948, (5) for 2012

period before 1948 for the shelf with depths less than 30 m (see Figure 1). An increase in the bottom water temperature during the period from 1948 to 2012 resulted in an insignificant (1–3 m) raising of the lower boundary permafrost.

In a previous study [27], we attempted to simulate the subsea permafrost of the ESAS since the Holocene transgression, i.e., since 8,000 years ago. It was assumed that the latest ocean transgression occurs simultaneously for the whole shelf and thus temporal changes of the transgression depending on the topography are not taken into consideration. The lower permafrost boundary for 1948 was 204 m on the whole shelf for the geothermal heat flux value of 60 mW/m^2 . In this experiment, the thickness of the frozen soil depends on the depth of the sea and makes up 170–320 m (Figure 2a). The recent distribution of the subsea permafrost thickness is characterized by the latitudinal zoning. The simulation results show that the greatest permafrost thickness should currently exist in the shallow shelf zone with a depth less than 30 m.

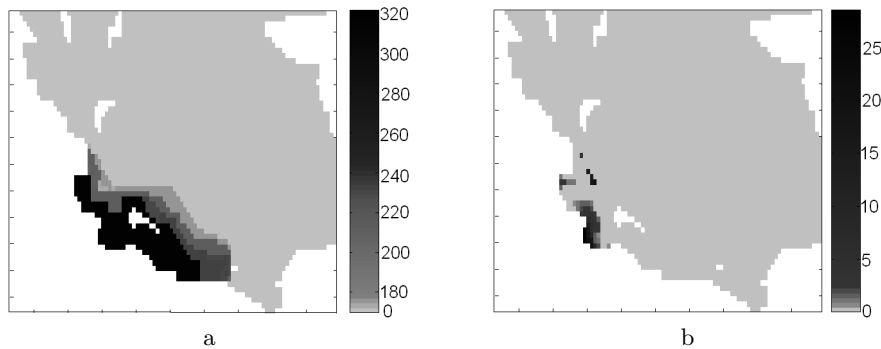


Figure 2. Simulated present-day permafrost (in m) for the heat flux of 60 mW/m^2 : (a) permafrost thickness in the ESAS, (b) locations of closed taliks in the ESAS

The mean annual temperatures of the bottom deposits are negative and make up 1.5°C . According to our computations, these conditions contribute to the thawing and formation of the closed submarine taliks (Figure 2b). The thawing at the upper boundary of the subsea permafrost in response to the bottom water temperature warming trend results in deepening the upper permafrost boundary. The results obtained show that by 2012 the upper boundary of the frozen sediment has deepened by 20–30 m in the shelf where the bottom water temperature becomes positive (see Figure 2b). The thawing from the sea floor is to occur in the offshore zone of the Laptev Sea eastward the Lena river delta, under the Dmitry Laptev Straite. The submarine permafrost degradation from above occurs most rapidly in the near-shore coastal zone of the shelf and in the areas affected by the Lena river outflow. Methane emissions may increase in the areas where the permafrost thawing results in significantly wetter soils. The microbial generating of methane in the permafrost sediments is so far an underestimated factor for the future climate development [28].

2.2. Response to a geothermal heat flux. According to [29], the geothermal heat flux within the Arctic shelf typically varies from 45 to 60 mW/m^2 and can reach 100 mW/m^2 in the areas of active zone. In this paper, we use the values of 45, 60, and 100 mW/m^2 to simulate the subsea permafrost dynamics within the ESAS.

The numerical results of the conducted experiments have demonstrated that the state of permafrost depends on the geothermal heat flux and the temperature profile is determined by heat flux. The simulation of the permafrost dynamics for different Q_T values shows that a maximum permafrost thickness is generally inversely proportional to the geothermal heat flux (Figure 3). The average permafrost thickness makes up around 330–490 m for a given heat flow of 45 mW/m^2 , around 170–320 m for a given heat flow of 60 mW/m^2 and around 0–95 m for a given heat flow of 100 mW/m^2 onto the ESAS. The rate of permafrost thawing is proportional to the Q_T value (see Figure 3b). It was established that the subsea permafrost thawing dynamics are more sensitive to the influence of the geothermal heat flux than to the top changes in bottom water temperature (Figure 4).

It is found that the open taliks should exist in the rift zones with high values of thermal flows (from 100 mW/m^2 and higher). These taliks have a local character and also depend on the bottom water temperature that is in agreement with the result [9]. Possible locations of open taliks on the Shelf, based on the 100 mW/m^2 flux obtained in the northwestern part of the Laptev Sea $\sim 119\text{--}123^{\circ}\text{E}$, 76°N . The continental slope is characterized by high values of the geothermal heat flux, and thus may tend to the development of open taliks. The open taliks may serve for the emission of the methane from the layers under the permafrost [8].

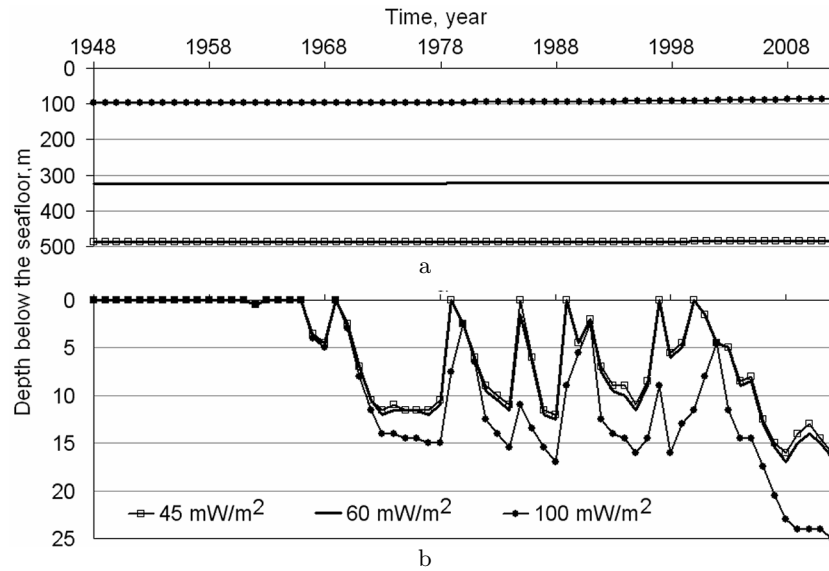


Figure 3. Simulated permafrost degradation after 1948 for a regional heat flux of 45, 60, and 100 mW/m²: (a) permafrost thickness, (b) the upper boundary of frozen sediments

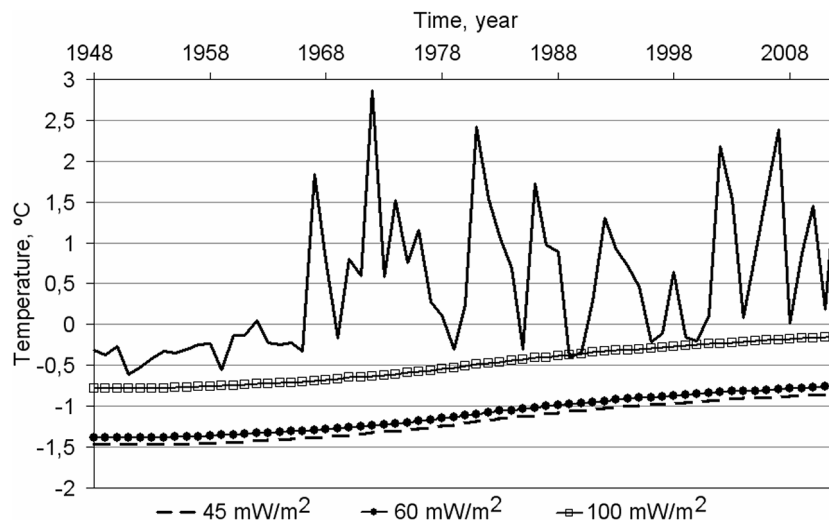


Figure 4. The summer seafloor temperature used as boundary condition for the Lena river delta (solid line) and the simulated summer ground temperature on the depth of 50 m below the seafloor for a regional heat flux of 45, 60, and 100 mW/m²

2.3. Gas hydrate stability zone: modeling results. Paper [4] declares CH_4 supersaturation in shallow ESAS coastal waters above sediments containing degrading subsea permafrost and presumably dissociating gas hydrates. In oceanic deposits, the depth at which hydrates remain stable depends on the pressure and the temperature. An increase in water temperature at the seafloor changes the extent of the GHSZ, and such a shift could induce hydrate dissociation and lead to methane release. The challenge lies in proving that at least some of the elevated methane concentrations detected in these settings are attributable to dissociating gas hydrates rather than to other processes associated with methane generation.

We explored the thickness of the Arctic seafloor GHSZ. The GHSZ is defined as the part of a sediment column where hydrostatic pressures are higher than the temperature dependent dissociation pressure of gas hydrates. The GHSZ appears on the shelf simultaneously with the development of subsea permafrost at cool climatic stages and then exists permanently in the transgression periods. The simulated thickness of the gas hydrate zone varied between 480 m to 670 m at the present time (Figure 5a). Temporal changes in the depth of the lower boundary of the hydrate stability zone occur in the same way as temporal variations in the depth of the lower boundary of the subsea permafrost. In the period of the sea transgression, the GHSZ is controlled not only by an increase in temperature, but also by changes in the excess pressure due to changes in the sea level.

The results of calculations illustrate that the upper boundary of the GHSZ over the East Siberian shelf regions lies within the permafrost at a depth 140–220 m below the seafloor (Figure 5b), which agrees with [5,6]. By increasing the bottom temperature, the GHSZ upper boundary descends and a possible hydrate decomposition occurs in the layer between its initial and current levels. The permafrost depth modeling shows a deepening down

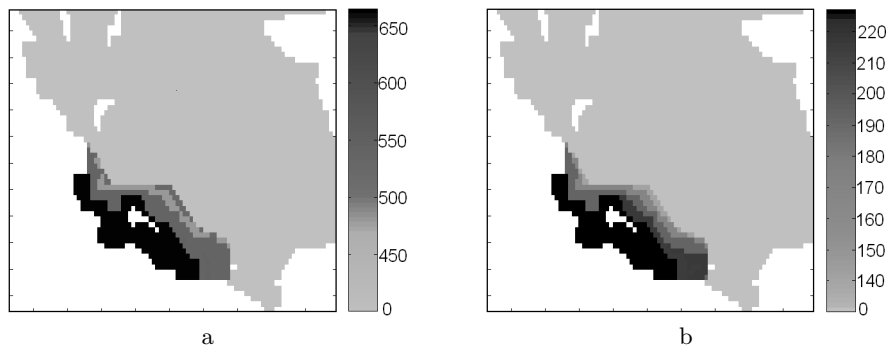


Figure 5. Simulated gas hydrate stability zone (in m) for 2012 for the heat flux of 60 mW/m^2 : (a) hydrate stability zone thickness in the ESAS, (b) locations of the upper boundary of the hydrate stability zone in the ESAS

to 30 m below the seafloor. This depth of the unfrozen permafrost is still less than that of the GHSZ upper boundary. The marine permafrost thawing in the rift zones with high values of thermal flows (from 100 mW/m² and higher) may be accompanied by the disappearance of the GHSZ, which may lead to increasing the methane emission into the sea water.

3. Conclusions

We numerically simulate the subsea permafrost evolution in the Arctic shelf in the Eastern Siberia for the last glacial cycle. The time of the transgression and regression cycles, the air temperature, the ocean bottom water temperature, the geothermal heat flux are some of the most important factors affecting the subsea permafrost dynamics. The numerical results obtained show that the offshore permafrost exists within the vast ESAS. This permafrost has a continuous character and its thickness varies across the Arctic shelf. The permafrost thickness within most of the East Siberian Arctic shelf is estimated as 170–320 m for a given a heat flow of 60 mW/m².

The permafrost thawing dynamics is most sensitive to the geothermal heat flux magnitude. The maximum permafrost thickness was generally inversely proportional to the geothermal heat flux. Open taliks can develop for a given geothermal heat flow exceeding 100 mW/m².

The permafrost thawing from the top depends on the seawater temperatures near the sea floor. The permafrost modeling shows that a significant change in the permafrost depth occurs with the seafloor warming in the Arctic Sea. The submarine permafrost degradation from above occurs most rapidly in the near-shore coastal zone of the shelf and in the areas affected by the Lena river outflow. Due to the warming of the oceans, an increasing release of methane can be expected to be a result of the permafrost melting. Methane emissions may increase in the areas where permafrost thaw results in significantly wetter soils [4, 8, 30, 31]

Currently, the calculated thickness of the gas hydrate stability zone makes up ≈ 600 m. The submarine permafrost plays the role of an impermeable lid and stops the motion of methane from destroyed gas hydrates, while it remains stable.

References

- [1] Polyakov I.D., Alekseev G.V., Bekryaev R.V., et al. Observationally based assessment of polar amplification of global warming // *Geophysical Research Letters*—2002.— Vol. 29, No. 18.— P. 25-1–25-4. doi:10.1029/2001GL011111.
- [2] Kwok R., Cunningham G.F., Wensnahan M., et al. Thinning and volume loss of the Arctic Ocean sea ice cover: 2003–2008 // *J. Geophys. Res.*— 2009.— Vol. 114.— C07005. doi:10.1029/2009JC005312.

-
- [3] Serreze M.C., Walsh J.E., Chapin F.S., et al. Observational evidence of recent change in the northern high-latitude environment // *Climatic Change*. — 2000. — Vol. 46. — P. 159–207.
- [4] Shakhova N., Semiletov I., Salyuk A., et al. Extensive methane venting to the atmosphere from sediments of the East Siberian Arctic Shelf // *Science*. — 2010. — Vol. 327. — P. 1246–1250. doi:10.1126/science.1182221.
- [5] Romanovskii N.N., Hubberten H.W., Gavrillov A.V., et al. Offshore permafrost and gas hydrate stability zone on the shelf of East Siberian Seas // *Geo Mar. Lett.* — 2005. — Vol. 25. — P. 167–182. doi:10.1007/s00367-004-0198-6.
- [6] Delisle G. Temporal variability of sub-sea permafrost and gas hydrate occurrences as function of climate change in the Laptev Sea, Siberia // *Polarforschung*. — 2000. — Vol. 68. — P. 221–225.
- [7] Gavrillov A., Romanovskii N., Romanovsky V., Hubberten H. Offshore permafrost distribution and thickness in the eastern region of the Russian Arctic, in *Changes in the atmosphere–land–sea system in the Amerasian Arctic* / I. Semiletov, ed. — Vladivostok, Russia: The Arct. Reg. Cent., 2001. — P. 209–218.
- [8] Shakhova N., Semiletov I., Leifer I., et al. Geochemical and geophysical evidence of methane release from the inner East Siberian Shelf // *J. Geophys. Res.* — 2010. — Vol. 115. — C08007. doi:10.1029/2009JC005602.
- [9] Nicolsky D.J., Romanovsky V.E., Romanovskii N.N., et al. Modeling sub-sea permafrost in the East Siberian Arctic Shelf: The Laptev Sea region // *J. Geophys. Res.* — 2012. — Vol. 117. — F03028. doi:10.1029/2012JF002358.
- [10] Osterkamp T. Subsea permafrost // *Encyclopedia of Ocean Sciences*. — San Diego, Calif.: Academic, 2001. — P. 2902–2912.
- [11] Nicolsky D., Shakhova N. Modeling sub-sea permafrost in the East Siberian Arctic Shelf: The Dmitry Laptev Strait // *Environ. Res. Lett.* — 2010. — Vol. 5. — 015006. doi:10.1088/1748-9326/5/1/015006.
- [12] Dmitrenko I., Kirillov S., Tremblay L., et al. Recent changes in shelf hydrography in the Siberian Arctic: Potential for subsea permafrost instability // *J. Geophys. Res.* — 2011. — Vol. 116. — C10027. doi:10.1029/2011JC007218.
- [13] Denisov S.N., Arzhanov M.M., Eliseev A.V., Mokhov I.I. Assessment of the response of subaqueous methane hydrate deposits to possible climate change in the twenty-first century // *Doklady Earth Sciences*. — 2011. — Vol. 441. — P. 1706–1709.
- [14] Kappelmeyer O., Haenel R. *Geothermics with Special Reference of Application* / *Geoexpl. Monographs*. — Berlin: Borntraeger, 1974. — S. 1, No 4.
- [15] Gavrillov A., Romanovskii N., Hubberten H.-W. Paleogeographical scenario of late-glacial transgression on the Laptev Sea shelf // *Earth Cryosphere*. — 2006. — Vol. 10, No 1. — P. 39–50.

- [16] Romanovskii N., Hubberten H.-W. Results of permafrost modeling of the lowlands and shelf of the Laptev Sea Region, Russia // *Permafrost Periglacial Processes*.— 2001.— Vol. 12, No 2.— P. 191–202.
- [17] Petit J., Jouzel J., Raynaud D., et al. Climate and atmospheric history of the past 420,000 years from the Vostok Ice Core, Antarctica // *Nature*.— 1999.— Vol. 399.— P. 429–436.
- [18] Kholodov A.L., Romanovskii N.N., Gavrilov A.V., et al. Modeling of the offshore permafrost thickness on the Laptev Sea shelf // *Polarforschung*.— 2001.— Vol. 69.— P. 221–227.
- [19] Bauch H.A., Mueller-Lupp T., Taldenkova E., et al. Chronology of the Holocene transgression at the North Siberian margin // *Global Planet. Change*.— 2001.— Vol. 31.— P. 125–139. doi:10.1016/S0921-8181(01) 00116-3.
- [20] Golubeva E.N., Platov G.A. Numerical modeling of the Arctic Ocean ice system response to variations in the atmospheric circulation from 1948 to 2007 // *Izvestiya. Atmospheric and Oceanic Physics*.— 2009.— Vol. 45, No. 1.— P. 137–151 (In Russian).
- [21] Golubeva E.N., Platov G.A. On improving the simulation of Atlantic Water circulation in the Arctic Ocean // *J. Geophys. Res.*— 2007.— Vol. 112.— C04S05. doi:10.1029/2006JC003734.
- [22] Kuzin V.I., Platov G.A., Golubeva E.N., Malakhova V.V. Certain results of numerical simulation of processes in the Arctic Ocean // *Izvestiya, Atmospheric and Oceanic Physics*.— 2012.— Vol. 48, No. 1.— P. 117–136.
- [23] *Review of Meteorological Processes in the Arctic Ocean*.— St. Petersburg: AARI, 2008.
- [24] Moridis G.J. Numerical studies of gas production from methane hydrates // *Society of Petroleum Engineers Journal*.— 2003.— Vol. 32, No. 8.— P. 359–370.
- [25] Sloan E.D. *Clathrate Hydrates of Natural Gases*.— New York: Marcel Dekker, Inc., 1998.
- [26] Moridis G.J., Kowalsky M.B., Pruess K. *Users Manual: a Numerical Simulator for Modeling the Behavior of Hydrates in Geologic media / HydrateResSim*. Department of Energy, Contract No. DE-AC03-76SF00098.— Lawrence Berkeley National Laboratory, Berkeley, CA, 2005.
- [27] Malakhova V.V. Mathematical modeling of the submarine permafrost long-term dynamics of the Arctic shelf // *Proc. Int. Conf. “Geo-Siberia-2014”*.— Novosibirsk: SGGa, 2014.— Vol. 1.— P. 136–140.
- [28] Wagner D., Gattinger A., Embacher A., et al. Methanogenic activity and biomass in Holocene permafrost deposits of the Lena Delta, Siberian Arctic and its implication for the global methane budget // *Global Change Biology*.— 2007.— Vol. 13.— P. 1089–1099. doi:10.1111/j.1365-2486.2007.01331.x.

- [29] Soloviev V., Ginzburg G., Telepnev E., Mikhailuk Y. Cryothermia and Gas Hydrates in the Arctic Ocean. — Leningrad: Sevmorgelgia, 1987.
- [30] Malakhova V.V., Golubeva E.N. The role of the Siberian rivers in increase of the dissolved methane concentration in the East Siberian shelf // Atmospheric and Oceanic Optics. — 2012. — Vol. 25, No. 6. — P. 534–538.
- [31] Malakhova V.V., Golubeva E.N. On possible methane emissions from the East Arctic Seas // Atmospheric and Oceanic Optics. — 2013. — Vol. 26, No. 6. — P. 452–458.